Journal of Natural Disaster Science, Volume 24, Number 2, 2002, pp91-100

Phase Spectrum Modeling to Simulate Design Earthquake Motion

Tadanobu SATO [1], Yoshitaka MURONO [2] and Akihiko NISHIMURA [2]
[1] Disaster Prevention Research Institute, Kyoto University, Kyoto, Japan
[2] Railway Technical Research Institute, Tokyo, Japan

(Received for 9. Oct., 2002)

ABSTRACT

Modeling the phase of earthquake ground motion is required in order to synthesize design ground motion that is compatible with the given response spectrum. A simple method is presented for modeling the phase characteristics of earthquake motion using the concept of group delay time and wavelet analysis. Using existing data sets of observed earthquake motions, we calculated the group delay time of each earthquake motion on each compact support of the mother wavelet. Because of the fluctuating nature of the group delay time on each support, the mean of the group delay times and standard deviation were calculated. Attenuation relations of the mean delay time and standard deviation on each support were obtained by regression analysis as functions of the earthquake's magnitude and epicentral distance. On the assumption that the group delay time has a normal distribution, a sample group delay time can be generated on each support, and by integrating it with respect to frequency the phase spectrum is derived. Simulated sample phase spectra were used to simulate earthquake motions compatible with a design response spectrum. Their characteristics were investigated using ductility demand spectra.

1. INTRODUCTION

Design earthquake motions often are defined by response spectra. For example, in the seismic design standards for the Japan Railway facilities (1999) there are two types of design spectra for level II earthquake motion: Spectrum I is defined by taking into account earthquake activities in the inter-plate region; Spectrum II is defined by considering the near source earthquake motion characteristics caused by intra-plate earthquakes. To assess the aseismic capacity of designed structures, dynamic analyses of structures must be made using earthquake motion compatible with the design response spectrum. The phase characteristics of earthquake motion as well as the amplitude therefore are important issues.

A primitive method developed in early stage studies of the simulation of design earthquake motions was to generate a nonstationary time history by multiplying an envelope function (Jennings,1969) to a stationary time history simulated using random phase criteria (Shinozuka and Jan,1972). Another method was to use the phase spectrum of a certain observed earthquake motion (Arakawa,1984). The phase characteristics of earthquake motions were not, however, clearly characterized by these methods.

Several pioneer works clarified the nonstationary characteristics of earthquake motion through analyses of its phase characteristics. Osaki (1978) showed similarity between the distribution width of the phase difference and the duration of earthquake motion. Izumi and Katsukura (1983) using the concept of group delay time, showed that the average arrival time of earthquake energy and duration of earthquake motion can be evaluated by the mean of group delay time and the standard deviation. Kimura (1986) presented a way to simulate earthquake motion by controlling the group delay time, but it was not based on observed earthquake motion data.

We developed a method to simulate the group delay time for near source earthquake motion by assuming that the rupture process of the earthquake fault can be expressed by a train of impulses and that the minimum phase concept is effective for evaluating the phase shift due to traveling pass (Sato, Murono and Nishimura, 1999). In that method only direct S wave motion was considered, the effect of surface wave motion on the group delay time was not taken into account. Moreover, to use the method detailed information on the fault rupture process and geological conditions of the transmitting path had to be given apriori.

The parameters that control the group delay time of earthquake motion therefore are modeled as a function of the epicentral distance, Δ, and earthquake magnitude, M, (i.e., the attenuation relationship) using observed earthquake motion data sets.

Several studies have developed the attenuation relationship related to the phase characteristics of earthquake motion. Sawada (1986) analyzed the phase difference of earthquake motions and derived an attenuation relationship for duration. Ishii (1987) derived attenuation relationships of the mean group delay time and its standard deviation for entire time history of earthquake motion. Satoh (1996) derived attenuation relationships of the mean group delay time and its standard deviation for fairly long period earthquake motion (period range 1-10s), using a wave form processed through a narrow band passed filter with the frequency of 0.02Hz.

The purpose of our study was to develop a model for simulating realistic group delay time of earthquake motion to be used for dynamic analyses of civil structural systems. The targeted frequency range was 0.2 to 10Hz. The general group delay characteristic is assumed to be modeled by the mean value and its standard

KEY WORDS:

deviation. We calculated these values for the wavelet-transformed earthquake motions on each compact support of the Meyer wavelet (Yamaguchi, 1990) and used regression analysis to derive the attenuation relationships of these values as functions of the epicentral distance, Δ, and earthquake magnitude, M. As an application we resimulated the earthquake motions of the Off Sanriku event (1995) and compared them with the observed earthquake motions. We also show the nonlinear response characteristics of a single degree of freedom structure to earthquake motions compatible with the design response spectrum defined in the Japan Railway design standards.

2. DATA BASE FOR THE ANALYSES

Earthquake motions were selected mainly from data sets recorded by the 87 type accelerometers of the Japan Meteorological Agency. Data sets distributed by the Kansai Earthquake Observation and Research Committee and the K-net of the Science and Technology Agency also were used. Earthquake motions that satisfy the following conditions were selected:

1) an earthquake magnitude larger than 6,
2) many observed data collectable from one event,
3) a hypocenter depth of less than 50km,
4) a maximum acceleration of more than 30 gal,
5) a sufficiently long duration.

Condition 1) was selected because our concern was to define the phase spectrum of level II earthquake motion. Condition 2) is needed to ensure homogeneous distribution of the earthquake observation data in the space of the earthquake's magnitude and epicentral distance. Condition 3) was needed for the selection of earthquakes that generate sufficient surface wave motion because such motion is not generated if the depth of the hypocenter is more than 50km. Condition 4) was required because if the maximum acceleration is less than 30 gal the S/N ratio will not be large enough to analyze the group delay time. Condition 5) was necessary to obtain observed earthquake motions over time until the arrival of the concerned wave with a targeted group velocity and frequency band.

Five recent earthquake data sets that satisfy the above conditions are given in Table 1. Figure 1 shows their distribution characteristics in the space of magnitude M and epicentral distance Δ. Earthquakes with long epicentral distances are those with large magnitudes, whereas those with short epicentral distances are only the 1995 Hyogoken Nambu (M7.2) and 1997 North-West Kagoshima Prefecture (M6.3) earthquakes.

Ground motions of the Off Southwest Hokkaido earthquake (1993, M7.8), the Off East Hokkaido earthquake (1994, M8.1) and the Off Sanriku earthquake (1994 M7.5) were recorded by the 87 type accelerometers of the Japan Meteorological Agency. The earthquake motions of the Hyogoken Nambu earthquake include records from both the Meteorological Agency and Kansai Earthquake Observation and Research Committee. All records for the Northwest Kagoshima event are from the K-net of the Science and Technology Agency.

3. ANALYTICAL METHOD

Data used for the analyses are the horizontal components of the observed earthquake motions.

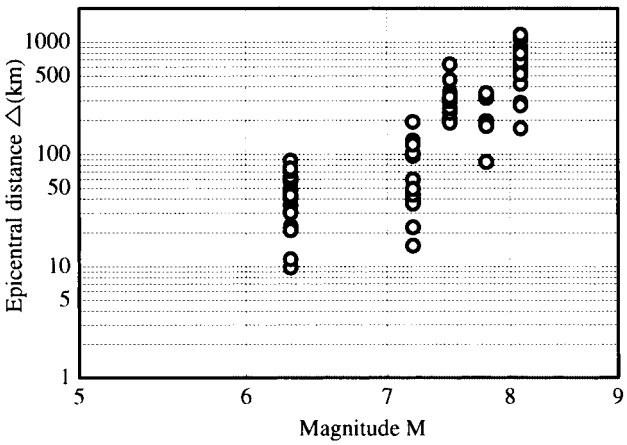

Fig. 1 Relationship between magnitude and epicentral Distance of the earthquake records used

3.1 Definition of Group Delay Time

Group delay time is defined by the derivative of the Fourier phase spectrum $\phi(\omega)$ with respect to circular frequency ω (Papoulis, 1962);

$$t_{gr}(\omega) = \frac{d\phi(\omega)}{d\omega} \tag{1}$$

The average value of the group delay time within a certain frequency band with the central frequency ω expresses the arrival time of a wave component with frequency ω. The distribution width of the group delay time is related to the duration of the time history of the wave component. Because of these characteristics of group delay time, its modeling is much easier than direct modeling of the phase spectrum.

The calculated Fourier phase spectrum $\phi(\omega)$ must be unlapped to obtain the group delay time based on equation (1). Izumi and Katsukura (1983) proposed a method to satisfy the condition $t_{gr} \geqq 0$, but the distribution of the group delay time is concentrated around the end of the time history of earthquake motion because of the rink effect. To eliminate this defect, an artificial zero time history was added (Satoh, 1996). Because the calculated group delay time depends on the number of data points in the time history, we applied the method of Sawada, Morikawa et al (1998), who showed that the calculated group delay time depends less on artificially added numbers of zeros to a time history of earthquake motion.

3.2 Average Group Delay Time and Its Standard Deviation

To show the nonstationary characteristic of earthquake motion in the time and frequency domains, wavelet analysis often is used because resolution in the time and frequency domains is guaranteed through the uncertainty criterion.

The discrete wavelet transformation of the function $x(t)$ and its inverse transformation were defined by (Yamaguchi, 1990)

$$a_{j,k} = \int_{-\infty}^{\infty} \psi^*_{j,k} \cdot x(t)\, dt \tag{2}$$

$$x(t) = \sum_j x_j(t) = \sum_j \sum_k a_{j,k} \cdot \psi_{j,k}(t) \tag{3}$$

$$\psi_{j,k}(t) = 2^{j/2} \cdot \psi(2^j t - k)\ j, k : \text{integer} \tag{4}$$

in which the value with the sign * expresses the complex conjugate of the original value, $\psi(t)$ the wavelet function, j the scale factor, and k the factor expressing the time shift. As seen from equation (4), if scale factor j becomes large the treating frequency range goes to the high frequency region. If the inverse wavelet transformation exists, $\psi(t)$ is called the analyzing wavelet. We used the method of Meyer (Meyer 1989) to compose $\psi(t)$ although there are several ways to define this function. The Fourier transformation of $\psi(t)$ has a compact support for each scale factor j (named the j th compact support) defined by

$$\{2^j / 3T_d \le f \le 2^{j+2}/3T_d\} \tag{5}$$

in which T_d (=NΔt, N: number of data, Δt: sampling interval) is the duration of earthquake motion.

For all oberved earthquake earthquake motions with a sampling interval of 0.01(sec) we added zero data until the total number of sampling data for each earthquake motion, N, became 131071 (=2^{17}). Using the wavelet transformation of each earthquake motion $x(t)$ we decomposed each time history of earthquake motion to a component time history of each scale factor j (j=1～17). We called this the jth component time history, $x^{(j)}(t)$. The group delay time of this time history, $t_{gr}{}^{(j)}(\omega)$, was calculated. Its mean, $\mu^{(j)}{}_{tgr}$, and standard deviation, $\sigma -^{(j)}{}_{tgr}$, on the jth compact support were then obtained from equations (6) and (7):

$$\mu_{tgr}^{(j)} = \sum_{i=1}^{N^{(j)}} \frac{t_{gr}^{(j)}(\omega_i)}{N^{(j)}} \tag{6}$$

$$\sigma_{tgr}^{(j)} = \sqrt{\frac{1}{N^{(j)}} \sum_{i=1}^{N^{(j)}} (t_{gr}^{(j)}(\omega_i) - \mu_{tgr}^{(j)})^2} \tag{7}$$

in which j=1,2⋯,17, $N^{(j)}$ is the number for the time history data at the jth scale factor defined by $N^{(j)}=2^j$, and $t_{gr}{}^{(j)}(\omega_i)$ the group delay time of the jth component time history at a circular frequency of ω_i as defined by equation (8);

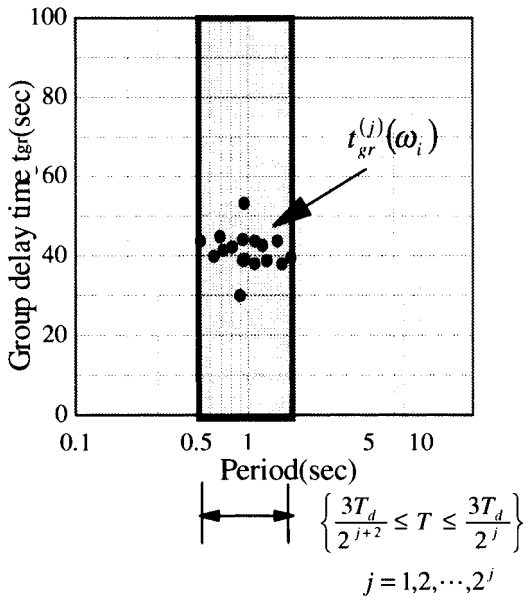

Fig. 2 Concept for calculating average group delay time and its standard deviation in each conpact support

$$\mu_{tgr}^{(j)} = \sum_{i=1}^{N^{(j)}} \frac{t_{gr}^{(j)}(\omega_i)}{N^{(j)}} \tag{8}$$

A sample calculation of these values is shown in Figure2.

4. NUMERICAL EXAMPLE

We used the proposed method to resimulate the earthquake motion records from the Morioka observation station for the 1993 Far-off Sanriku earthquake.

An example of earthquake motion decomposed into each component time history $x^{(j)}(t)$ is shown in Figure 3. As scale factor j becomes smaller, the duration lengthen and the central arrival time of the component time history is delayed. The Fourier amplitude spectrum on each compact support, $A^{(j)}(\omega)$, is shown in Figure 4. The Fourier amplitude on the jth compact support overlaps the Fourier amplitudes on both the (j-1)th and (j+1)th compact supports because the definition of the jth support is given by equation (5). The main frequency range in which the Fourier amplitude on the jth compact support predominates, is given by

$$\{2^{j-1} / T_d \le f \le 2^j / T_d\} \tag{9}$$

The vertical broken line in Figure 4 shows the frequency range defined by this equation.

Values of $\mu^{(j)}{}_{tgr}$ and $\sigma^{(j)}{}_{tgr}$ for the jth component time history $x^{(j)}(t)$ based on equations (6) and (7) are shown in Figure 5. The group delay time $t_{gr}(\omega)$ calculated from the observed time history of the earthquake motion also is shown. The values $\mu^{(j)}{}_{tgr}$ and $\sigma^{(j)}{}_{tgr}$ well indicate the group delay time of the observed earthquake motion. Comparison of Figures 3 and 5 shows that the central

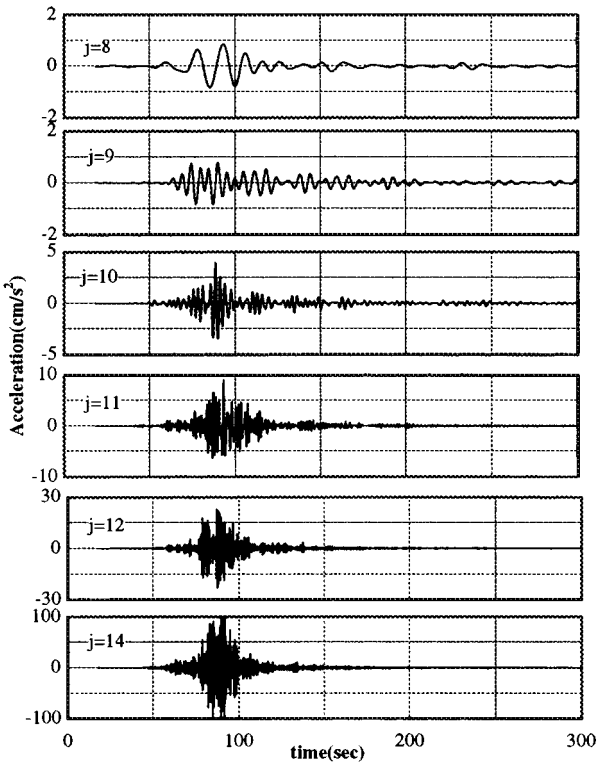

Fig. 3 Wavelet decomposed time histories for each scale factor j

arrival time of the *j*th component time history coincides with $\mu^{(j)}_{tgr}$ and that the duration is well evaluated by $\sigma^{(j)}_{tgr}$.

The distribution of group delay time on each compact support is shown in Figure 6. The examples for *j*=9 and 11 have the character of a normal distribution. When the value of *j* become small, the distribution character is distorted and approaches a log normal distribution. This tendency is confirmed by the fact that the envelop functions for cases of *j*=8,9 close to the log normal distribution function (Figure 3). We assume, however, that the values for group delay time have the normal distribution characteristic for all *j* values.

Earthquake motion resimulated using the average value of the group delay time, $\mu^{(j)}_{tgr}$, and its standard deviation, $\sigma^{(j)}_{tgr}$, is shown in Figure 7. We compared the resimulated motion with the observed one. The group delay time $_{tgr}{}^{(j)}(\omega)$ for the *j*th component time history on the compact support $\{2^j/3T_d \leqq f \leqq 2^{j+2/}3T_d\}$ is generated by assuming the normal distribution of $N(\mu^{(j)}_{tgr}, \sigma^{(j)}_{tgr})$. Integration gives the phase spectrum for the *j*th component time history, $x^{(j)}(t)$. The Fourier amplitude spectrum, $A^{(j)}(\omega)$, on the *j*th compact support is assumed to coincide with the Fourier amplitude of the observed earthquake motion, $A(\omega)$, in the frequency range $\{2^{j-1}/T_d \leqq f \leqq 2^j/T_d\}$ and to be zero outside of this region; i.e., in the frequency regions of $\{2^j/3T_d \leqq f < 2^{j-1}/T_d\}$ and $\{2^j/T_d < f \leqq 2^{j+2}/3T_d\}$.

We used this kind of simplicity because our purpose was not to model the Fourier amplitude on the compact support. Using the calculated $\phi^{(j)}(\omega)$ and modeled $A^{(j)}(\omega)$ for *j*=1～17, we resimulated each component time history and obtained the earthquake motion by summing up all the *j*th component time histories. A comparison of the resimulated motion with the observed one is shown in Figure 7, as is the simulated group delay time. The overall trend of the simulated group delay time agrees well with that of the observed earthquake motion. Group delay time calculated from the observed motion has a much wider distribution than the simulated one in the period range of 3-10sec because a normal distribution was assumed for all the *j*th component group delay times. The shapes of the simulated time histories of acceleration and displacement, however, agree well with those of the observed ones.

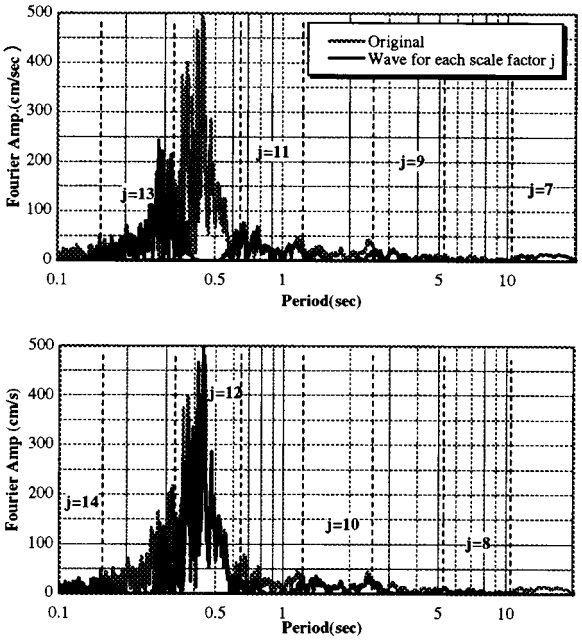

Fig. 4 Fourier amplitude $A^{(j)}(\omega)$ for each compact support j

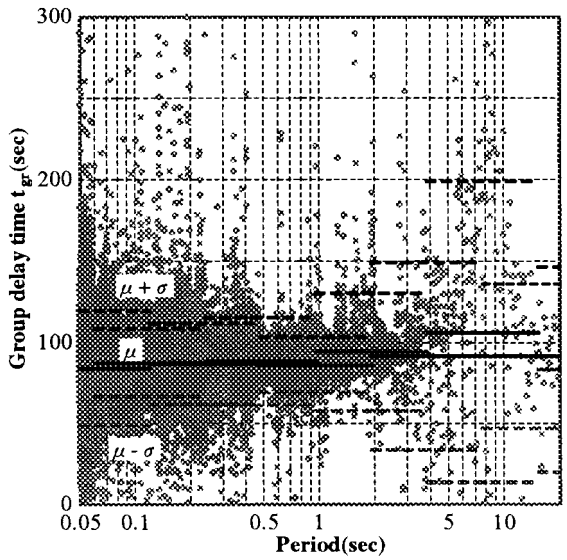

Fig. 5 Average group delay time μ_{tgr} and its standard deviation σ_{tgr} in each compact support

5. MODELING OF GROUP DELAY TIME

The mean group delay time, $\mu^{(j)}_{tgr}$, and its standard deviation, $\sigma^{(j)}_{tgr}$, were calculated for all the observed earthquake motions listed in Table 1. Because the trigger time of earthquake motion is recorded in all the observation data, the time origin of earthquake motion was defined by adding the theoretically calculated travel time of the direct S wave generated at the initial rupture point on the earthquake fault to the trigger time. The concerned period range in standard aseismic design procedures is 0.1-5 sec. The

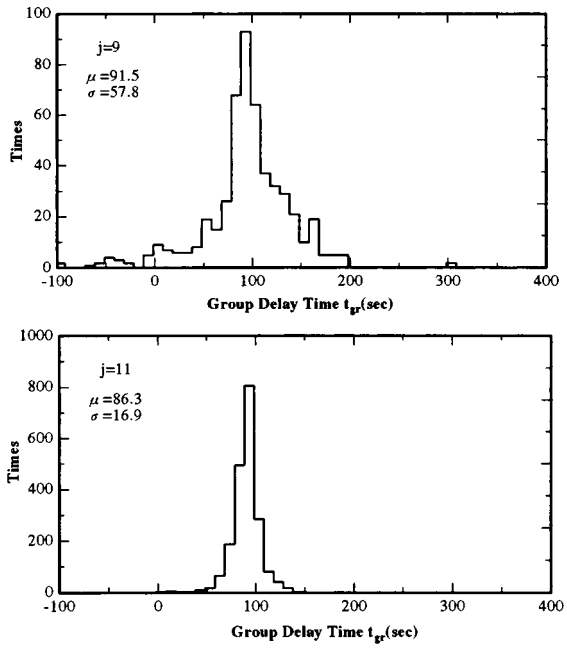

Fig. 6 Distribution characteristics of group delay time $t_{gr}(\omega)$ on compact support j = 9, 11

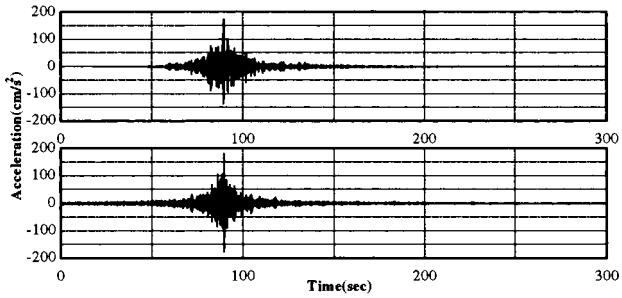

(a) time history of acceleration (Upper: Observed, Lower: Simulated)

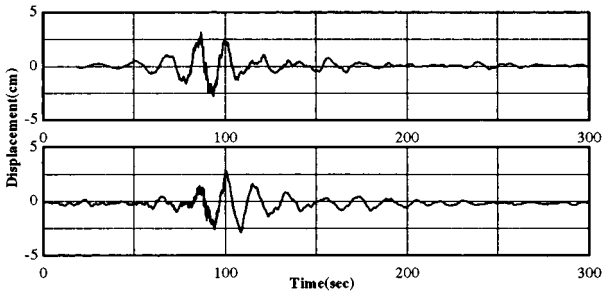

(b) time history of displacement (Upper: Observed, Lower: Simulated)

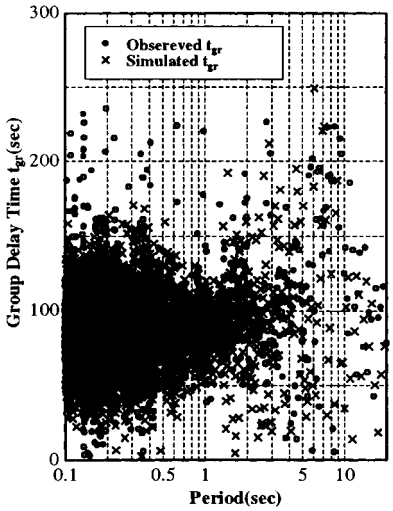

(c) Group delay time

Fig. 7 Comparison with observed and simulated motions

Table 1. Earthquake data sets used

Earthquake	Magnitude M	number of data sets
Hokkaido Nansei Oki (1993)	7.8	10 data
Hokkaido Toho Oki (1994)	8.1	42 data
Sanriku Haruka Oki (1994)	7.5	26 data
Hyogoken Nanbu (1995)	7.2	28 data
Kagoshimaken Hokuseibu (1997)	6.3	26 data

Table 2. Regression analyses results

j	α_1	α_2	β_1	β_2	γ_1	γ_2
7	1.011	27.708	0.0	0.0	0.864	0.203
8	0.830	14.584	0.040	0.0	0.790	0.337
9	0.543	17.968	0.086	-0.030	0.700	0.344
10	0.806	8.451	0.060	-0.005	0.686	0.321
11	0.850	2.970	0.026	0.016	0.764	0.366
12	0.511	0.392	0.058	0.143	0.744	0.295
13	0.367	0.0790	0.077	0.267	0.739	0.201
14	0.330	0.0572	0.081	0.287	0.742	0.239
15	0.0443	0.0106	0.256	0.439	0.591	0.204

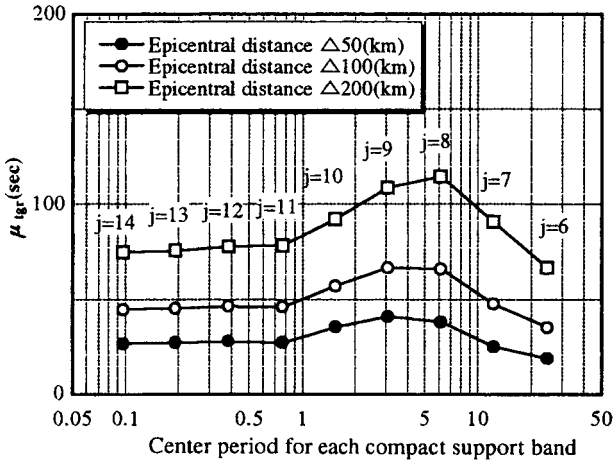

Fig. 8 Period dependence of average group delay times

attenuation relations $\mu^{(j)}_{tgr}$ and $\sigma^{(j)}_{tgr}$ for j=7-14 therefore were developed as functions of earthquake magnitude M and epicentral distance Δ (km).

$$\mu^{(j)}_{tgr} = \alpha_1^{(j)} \times 10^{\beta_1^{(j)} M} \times \Delta^{\gamma_1^{(j)}} \tag{10}$$

$$\mu^{(j)}_{tgr} = \alpha_1^{(j)} \times 10^{\beta_1^{(j)} M} \times \Delta^{\gamma_1^{(j)}} \tag{11}$$

in which $\alpha^{(j)}$, $\beta^{(j)}$ and γ (j) are regression coefficients on the jth compact support. Regression analysis results are shown in Table 2 and Figures 8 and 9. The β values for j=7-8 are forced to be zero because in this range β has small negative values which means that the arrival time of the jth component time history $x^{(j)}(t)$ becomes earlier and the duration longer for the smaller the earthquake magnitude. These characteristics have no physical meaning, rather they are due to the scattering of data. The effective number of data on the jth compact support is given by

$$N^{(j)} = 2^j \tag{12}$$

As the number of data on the compact support for j=7-8 was insufficient, large scattering occurred. The respective values of the correlation coefficients μ_{tgr} and σ_{tgr} are 0.9 and 0.71～0.87 (less than 0.5 for j=7).

The value of $\mu^{(j)}_{tgr}$ becomes larger as the epicentral distance increases. The regression coefficient γ_1 has a constant range of 0.68-0.8 for all orders of j. This means that the arrival times of all the component time histories ($x^{(j)}(t)$, j=7-14) are delayed as the transmitting path lengthens. Because the value of β_1 is less than 0.1, the effect of epicentral distance on the average group delay time is relatively greater than that of earthquake magnitude. The value of $\mu^{(j)}_{tgr}$ depends on the value of j; i.e., the average arrival time of the component time history is frequency dependent (Figure

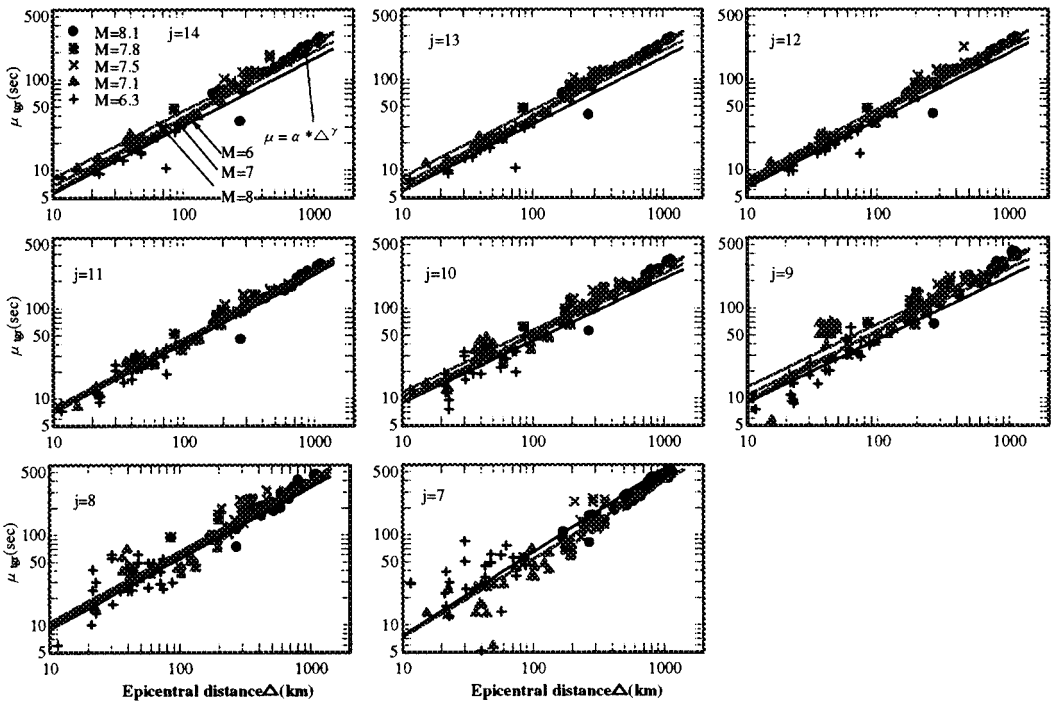

(a) Average group delay time μ_{tgr}

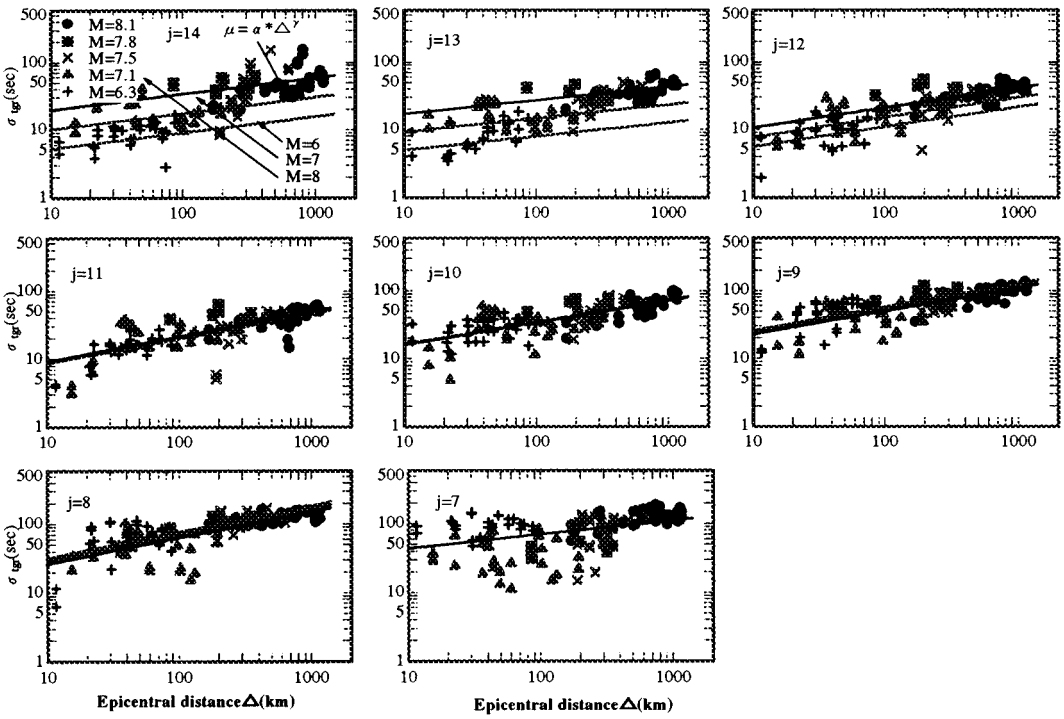

(b) Standard deviation of group delay time σ_{tgr}

Fig. 9 Average group delay time, its standard deviation in earthquake records, and regression analysis results

8) .

The duration of the *j*th component time history could be evaluated from the value of $\sigma_{tgr}^{(j)}$. As the order of *j* increases the value of γ_2 becomes smaller and β_2 larger. The surface wave predominates in the low frequency range of less than 1Hz, whereas the body wave has its main components in the high frequency range of 1-several Hz. Characteristics of the regression coefficients therefore are interpreted as follows: In the frequency region dominated by the body wave ($j \geqq 12$), the duration of the component time history is determined mainly by earthquake magnitude, whereas in the surface wave region ($j \leqq 11$) the effect of epicentral distance on its duration becomes larger than that of earthquake magnitude.

Two controversial studies related to the effect of epicentral distance on the duration of earthquake motion have been reported.

One (Trifunac, 1975) supports a strong effect, the other is against it (Kamiyama, 1984).

Sato and Uetake *et al*. (1996) concluded that the effect of earthquake magnitude on the mean group delay time and its standard deviation is very small. Our findings for the mean group delay time support their conclusion because the value of β_1 is smaller than 0.1. The difference in standard deviations between our and their results is because they analyzed only long period motion. The value of β_2 approaches zero in our research when the value of j becomes smaller than 10 (period lager than 1.04sec), which is consistent with their conclusion.

Table 1. Earthquake data sets used

j	α_1	α_2	γ_1	γ_2
7	1.011	27.71	0.864	0.203
8	1.338	14.58	0.831	0.337
9	1.517	12.53	0.786	0.314
10	1.644	7.988	0.746	0.317
11	1.155	3.597	0.790	0.382
12	1.026	2.138	0.802	0.438
13	0.915	1.891	0.816	0.468
14	0.866	1.743	0.823	0.526
15	0.931	1.957	0.847	0.643

The attenuation relation of each component time history, neglecting the effect of earthquake magnitude, also was obtained by assuming equations (13) and (14). Regression analysis results are given in Table 3 and shown by bold lines in Figure 9.

$$\mu_{tgr}^{(j)} = \alpha_1^{(j)} \times \Delta^{\gamma_1^{(j)}} \tag{13}$$

$$\sigma_{tgr}^{(j)} = \alpha_2^{(j)} \times \Delta^{\gamma_2^{(j)}} \tag{14}$$

6. VERIFICATION OF ATTENUATION RELATION

To verify the proposed modeling method of the phase spec-

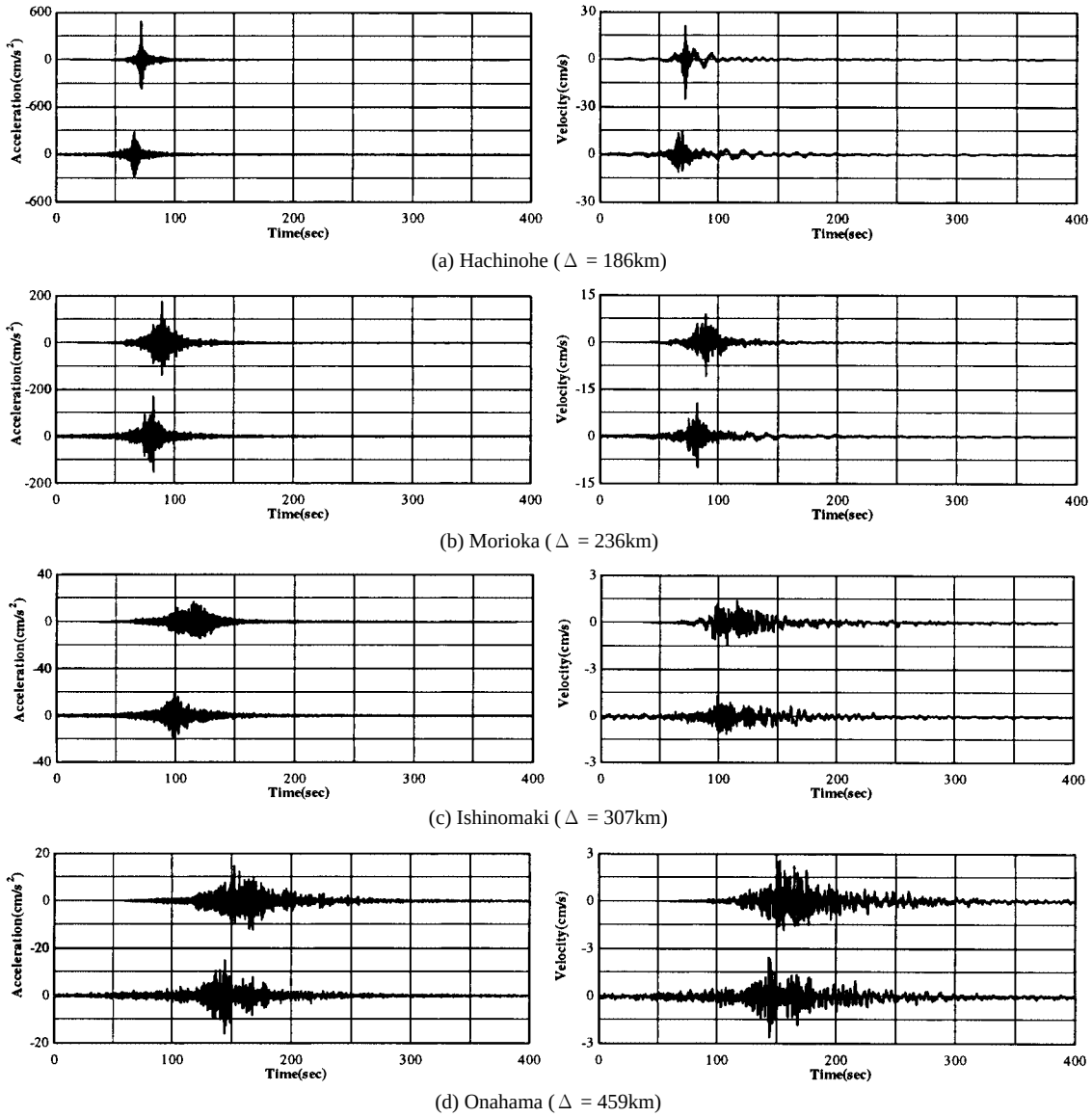

(a) Hachinohe (Δ = 186km)

(b) Morioka (Δ = 236km)

(c) Ishinomaki (Δ = 307km)

(d) Onahama (Δ = 459km)

Fig. 10 Comparison of observed and simulated motions using the proposed model (Upper: Observed, Lower: Simulated)

trum we simulated earthquake motions recorded during the 1994 Far-off Sanriku earthquake at the Hachinohe (Δ=186km), Morioka (Δ=236km), Ishinomaki (Δ=307km) and Onahama (Δ=459km) observation stations.

We targeted the EW components. Fourier amplitudes on the jth compact support $A^{(j)}(\omega)$ were defined as in section 4 using the observed Fourier amplitudes, $A(\omega)$. From the given earthquake magnitude and epicentral distance we calculated $\mu^{(j)}_{tgr}$ and $\sigma_{(j)tgr}$. The group delay time on jth compact support $t_{gr}^{(j)}(\omega)$ was simulated by generating random values based on the normal distribution, N ($\mu^{(j)}_{tgr}$, $\sigma^{(j)}_{tgr}$). The phase spectrum $\phi^{(j)}(\omega)$ was obtained by integrating $t_{gr}^{(j)}(\omega)$ with respect to ω. The acceleration time histories composed from $\phi^{(j)}(\omega)$ and $A^{(j)}(\omega)$ and the velocity time histories are shown in Figure 10. The central arrival time and duration of earthquake motions agree well with the observed motions. The non-stationary arrival characteristic of the wave group also agrees well with observed earthquake motions.

7. EARTHQUAKE MOTIONS COMPATIBLE WITH THE DESIGN RESPONSE SPECTRUM

Earthquake motions compatible with the design response spectrum defined in the earthquake-resistant design standard of the Japan Railway facilities were simulated (Figure 11). The values of the average group delay time $\mu^{(j)}_{tgr}$ and standard deviation $\sigma^{(j)}_{tgr}$ on the jth compact support were obtained for an earthquake of magnitude 8.0 and several epicentral distances (10, 100, 300 km) using the attenuation relationship developed in section 4. The phase spectrum on the jth compact support $\phi^{(j)}(\omega)$ was simulated using these two values. To simulate an earthquake motion compatible with the response spectrum, an initial Fourier amplitude spectrum $A_{int}(\omega)$ is needed. This is assumed to be given by the velocity response spectrum with zero damping coefficient converted from the design acceleration response spectrum as shown in equation (15).

$$A_{int}(\omega) = \left(\frac{\beta}{1+\alpha h} + \gamma\right) \omega S(\omega, 0.05) \qquad (15)$$

in which $S(\omega, 0.05)$ is the targeted design spectrum with 5% damping, h the damping constant, and α, β and γ given parameters (Kwashima and Aizawa, 1986)

The initial Fourier amplitude of the jth compact support $A^{(j)}(\omega)$ is assumed to coincide with the initial Fourier amplitude $A_{int}(\omega)$ in the frequency range $\{2^{j-1}/T_d \leqq f \leqq 2^j/T_d\}$ and to be zero outside of this region; i.e., in the frequency regions $\{2^j/3T_d \leqq f < 2^{j-1}/T_d\}$ and $\{2^j/T_d < f \leqq 2^{j+2}/3T_d\}$. A jth component time history can be simulated using $\phi^{(j)}(\omega)$ and $A^{(j)}(\omega)$. Earthquake motion of the first step is obtained by summing up all the component time histories. Because the calculated response spectrum based on first step earthquake motion does not coincide with the design response spectrum, we modified the amplitude of the initial Fourier amplitude, $A_{int}(\omega)$, at the circular frequency, ω, by multiplying the ratio $r(\omega)$ between the design response spectrum and the calculated response spectrum. Assuming the calculated $r(\omega)\, A_{int}(\omega)$ to be the new initial Fourier amplitude of earthquake motion and using the original phase spectrum of the jth component $\phi^{(j)}(\omega)$, we could simulate the earthquake motion of the second step. By repeating this process until ratio $r(\omega)$ nealy approached 1.0, we finally could simulate earthquake motion compatible with the design response spectrum.

The simulation results are shown in Figure 12. The design response spectrum shown in Figure 11 was defined by taking into account only the activity of inter-plate earthquakes (Wang, 1999). The epicentral distance for these earthquakes in Japan therefore is more than 30-40 km, so we added the case of a 10 km epicentral distance to compare the general characteristics of the simulated

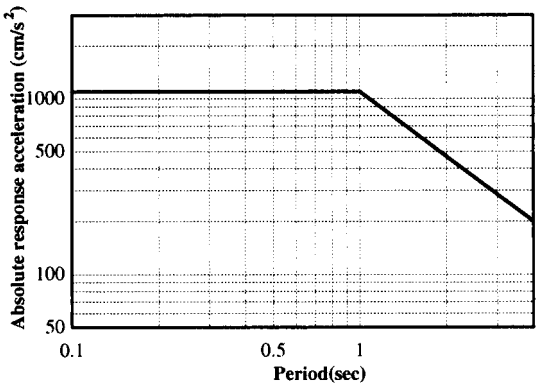

Fig. 11 The design response acceleration spectrum defined in the earthquake resistance design standards of Japan Railway Companies

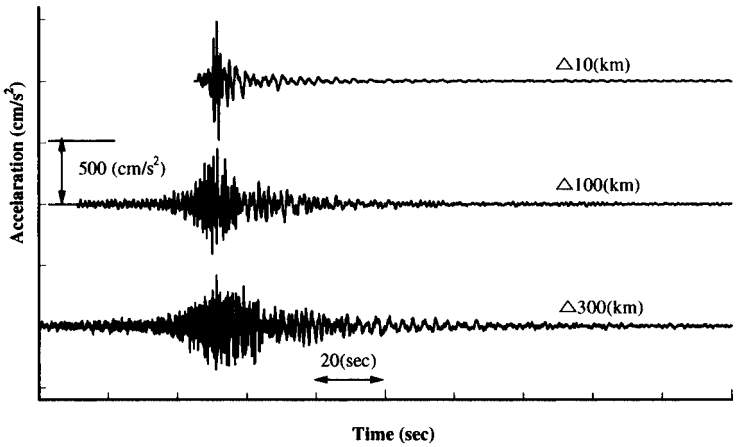

Fig. 12 Earthquake motions compatible with the design response spectrum in figure 11.

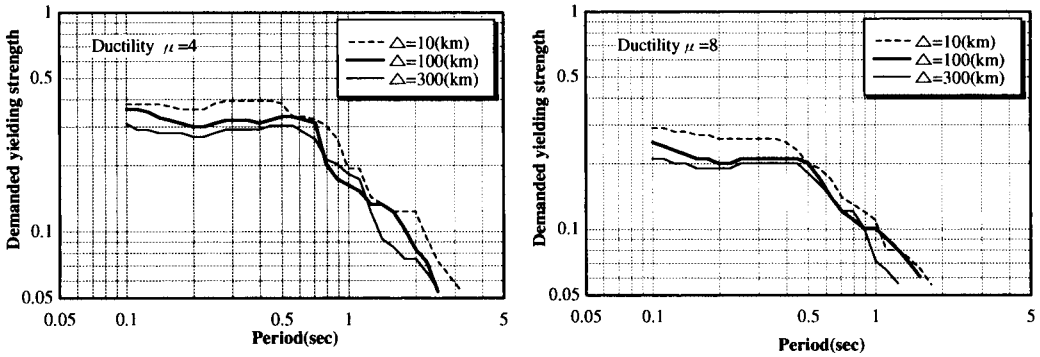

(a)Ductility μ =4 (b) Ductility μ =8

Fig. 13 Ductility demand spectrum for earthquake motions compatible with the response spectrum in figure 11

earthquake motions. In this case, the simulated earthquake motion shows such typical near-source motion characteristics as a short duration and pulse-like wave form. As the epicentral distance increases, the duration lengthens and longer period motion predominates in the latter part of the earthquake motion.

We calculated the ductility demand response spectra using the simulated earthquake motions shown in Figure 13. The ductility demand spectrum was obtained through nonlinear dynamic response analyses of a single degree of freedom system. The yield seismic coefficient of the SDF is controlled until the SDF response reaches the targeted ductility. The chart that expresses the relationship between the yield seismic coefficient and elastic natural period is called the ductility demand spectrum, in which the targeted ductility is a parameter. The hysteresis model used for the analyses is a bi-linear type of model proposed by Clough (1966). The second stiffness is selected as 5% of the first, and a 5% damping coefficient assigned. Although we used the same elastic response spectrum to simulate the earthquake motions, the strong effect of epicentral distance can be seen on the elasto-plastic structural response characteristics. A shorter epicentral distance demands a large ductility whereas the demand decreases as the epicentral distance increases.

8. CONCLUSION

A method for modeling the phase spectrum of earthquake motion is proposed that is based on the concept of group delay time. The findings of this study are

1) By using data sets of observed earthquake motions and the wavelet algorithm, the average group delay time and standard deviation on the compact support of Mayer wavelet can be expressed as functions of earthquake magnitude and epicentral distance.
2) By use of derived attenuation relationship, earthquake motions at sites where earthquake motions were recorded during the 1994 Far-off Sanriku earthquake could be simulated. The simulated motions agreed well with the characteristics of the recorded motions.
3) A method to simulate earthquake motion compatible with the design response spectrum was developed. Its suitability for design purposes was investigated using ductility demand spectra.

ACKNOWLEDGEMENT

We gratefully acknowledge the computer program for wavelet analysis provided by Professor M. Yamada from University of Tokyo.

APPENDIX REFERENCES

1) Arakawa, T., Kawashima, K. and Aizawa, K. (1984). “Input ground motions for step-by-step integration dynamic response analysis by modifying response spectral characteristics”, *Civil Engineering Journal*, Vol.26, No.7 (in Japanese).
2) Clough, R. W. and S. B. Johnston, S. B. (1966). “Effect of stiffness degradation on earthquake ductility requirements”, *Proc. the 2nd Japan Earthquake Engineering Symposium*, 227-232.
3) Ishii, T. and Watanabe, T. (1987). “Relation between phase characteristics of ground motions and magnitudes, focal distances and focal depths of earthquakes”, *Summaries of Technical Papers of Annual Meetings of AIJ, Structures I*, 385-386 (in Japanese).
4) Jennings, P. C., Housner, G. W. and Tstai, N. C. (1968). “Simulated earthquake motions for design purpose”, *Proc. of 4-th World Conference on Earthquake Engineering*, 145-160.
5) Kamiyama, M. (1984). “A statistical analysis of duration and its related parameters with emphasis on soil conditions”, *J. Struct. Mech. Earthquake Eng., JSCE*, No.350/I-2, 271-280 (in Japanese).
6) Katukura, K. and Izumi, M. (1983). “A fundamental study on the phase properties of seismic waves”, *J. Struct. Constr. Eng., Transactions of AIJ.*, No.327, 20-27 (in Japanese).
7) Kawashima, K. and Aizawa, K. (1986). “Modification of earthquake response spectra with respect to damping”, *J. Struct. Mech. Earthquake Eng., JSCE*, No.344/I-1, 351-355 (in Japanese).
8) Kimura, M. (1986). “On control of the characteristics of the wave in generating simulated earthquake ground motions”, *J. Struc. Constr. Eng., Transactions of AIJ.*, No.367, 30-36 (in Japanese).
9) Meyer, Y. (1992). “Wavelets and Operators”, Cambridge University Press.
10) Ohsaki, Y., Iwasaki, R., Okawa, I., and Masao, T. (1978). “A study on phase characteristics of earthquake motions and its applications”, *Proc. the 5th Japan Earthquake Engineering Symposium*, 201-208 (in Japanese).
11) Papoulis, A. (1962). “The Fourier integral and its application”, McGraw-Hill.

12) Railway Technical Research Institute (1999). “Seismic design code for railway structures”, Tokyo (in Japanese).
13) Sasaki, F., Maeda, T. and Yamada, M. (1992). “Study of time history data using wavelet transform”, *J. Struc. Eng., AIJ*, Vol.38B, 9-20 (in Japanese).
14) Sato, T., Murono, Y. and Nishimura A. (1999). “Modeling of phase characteristics of strong earthquake motion”, *J. Struct. Mech. Earthquake Eng., JSCE*, No.612/I-46, 201-213 (in Japanese).
15) Satoh, T., Uetake, T. and Sugawara, Y. (1996). “A study on envelope characteristics of strong motions in a period range of 1 to 15 seconds by using group delay time”, *Proc. of World Conference on Earthquake Engineering, Paper No.149*,
16) Sawada, S., Morikawa, H., Toki, K. and Yokoyama, K. (1998). “Identification of path and local site effects on phase spectrum of seismic motion”, *Proc. 10th Japan Earthquake Engineering Symposium*, 915-921 (in Japanese).
17) Sawada, T., Nagae, M. and Hirao, K. (1986), “A definition for duration of earthquake ground motion by phase differences and its statistical analysis”, *J. Struct. Mech. Earthquake Eng., JSCE*, No.368/I-5, 373-382 (in Japanese)
18) Shinozuak, M and Jan C.-M. (1972). “Digital simulation of random proceses and its applications”, *Journal of Sound and Vibration*, Vol.25, No.1, 111-128.
19) Trifunac, M.D. and Brady, A.G. (1975). “A study on the duration of strong earthquake ground motion”, *Bull. Seis. Soc. Am.*, Vol.65, No.3, 581-626.
20) Yamaguchi, M. and Yamada, M. (1990) “Wavelet analysis”, *Science*, Vol.60 No.6, 398-405 (in Japanse).
21) Wang, H., Nishimura, A. and Naganawa, T. (1999). “Seismic motion level in acceleration response spectra on engineering bedrock”, *RTRI REPORT*, Vol.13, No.2, 11-18 (in Japanese).